Supporting Information

In-situ Studies of Molecular Packing Dynamics of Bulk-heterojunction Solar Cells induced by the Processing Additive 1-Chloronaphthalene

Sooncheol Kwon[a,b,†], Jin Kuen Park[c,†], Jehan Kim[d,†], Geunjin Kim[a,b], Kilho Yu[a,b], Jinho Lee[a,b], Yong-Ryun Jo[a], Bong-Joong Kim[a], Hongkyu Kang[a,b], Junghwan Kim[a,b], Heejoo Kim[b,*] and Kwanghee Lee[a,b,*]

[a] School of Materials Science and Engineering, Gwangju Institute of Science and Technology, Gwangju 500-712, Korea
[b] Heeger Center for Advanced Materials (HCAM) & Research Institute for Solar and Sustainable Energies (RISE), Gwangju Institute of Science and Technology, Gwangju 500-712, Korea
[c] Departments of Chemistry, Hankuk University of Foreign Studies, Yongin 449-791, Republic of Korea
[d] Pohang Accelerator Laboratory (PAL), Pohang University of Science and Technology (POSTECH), Pohang 790-784, Republic of Korea
*Address correspondence to heejook@gist.ac.kr, klee@gist.ac.kr.

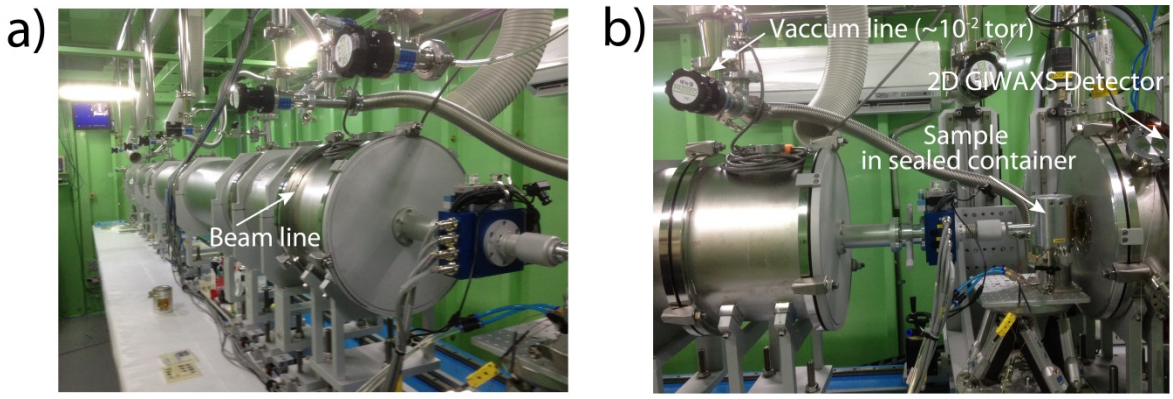

Figure S1. The 3C SAXS I beam line at Pohang Accelerator Laboratory (PAL), used for this study of the molecular packing dynamics of the P1:$PC_{71}BM$ BHJ blend system through *In-situ* GIWAXS measurement.

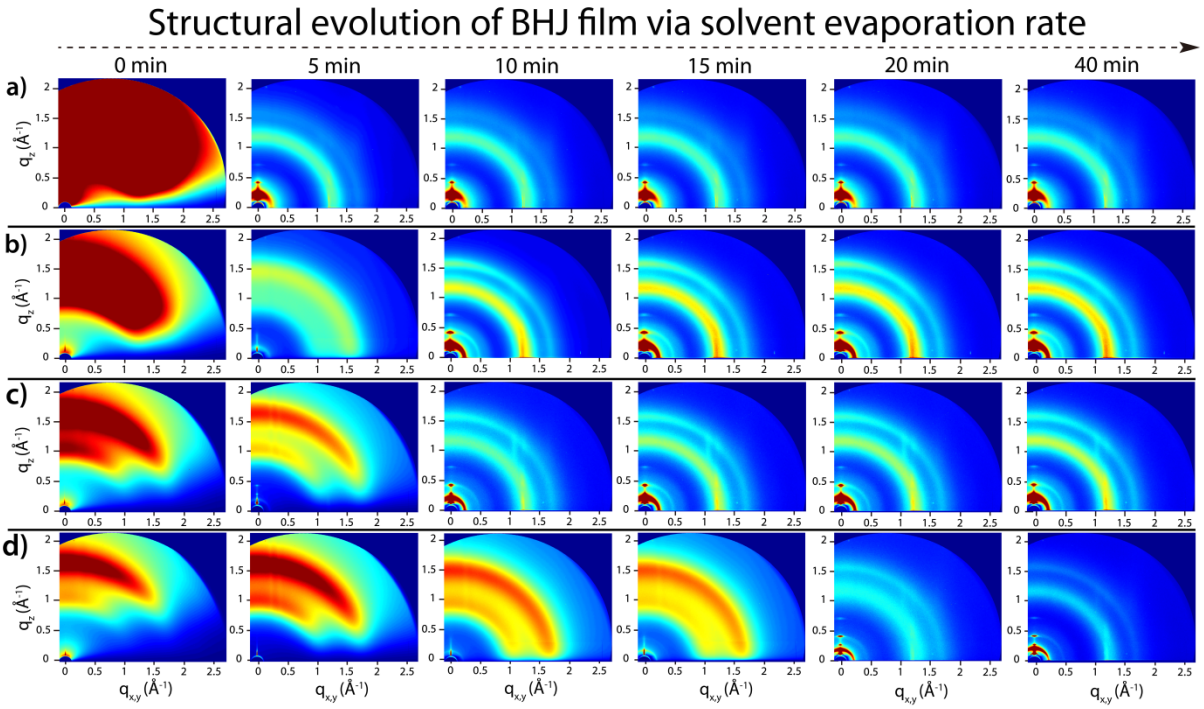

Figure S2. Real-time 2D GIWAXS patterns obtained during drying of P1:$PC_{71}BM$ cast on Si substrate with solvents of a) CB, b) CB+1-CN, c) DCB and d) DCB+1-CN at a temperature of 25 ºC. The initial state of each sample displays the solvent evaporation, and the film drying of the subsequent evolutions in the samples was slower on the high order of the boiling point of the solvent (boiling point: DCB+1-CN > DCB > CB+1-CN > CB), resulting in the different structural evolutions of the P1:$PC_{71}BM$ BHJ film. Above the 2D GIWAXS images, the drying times are indicated.

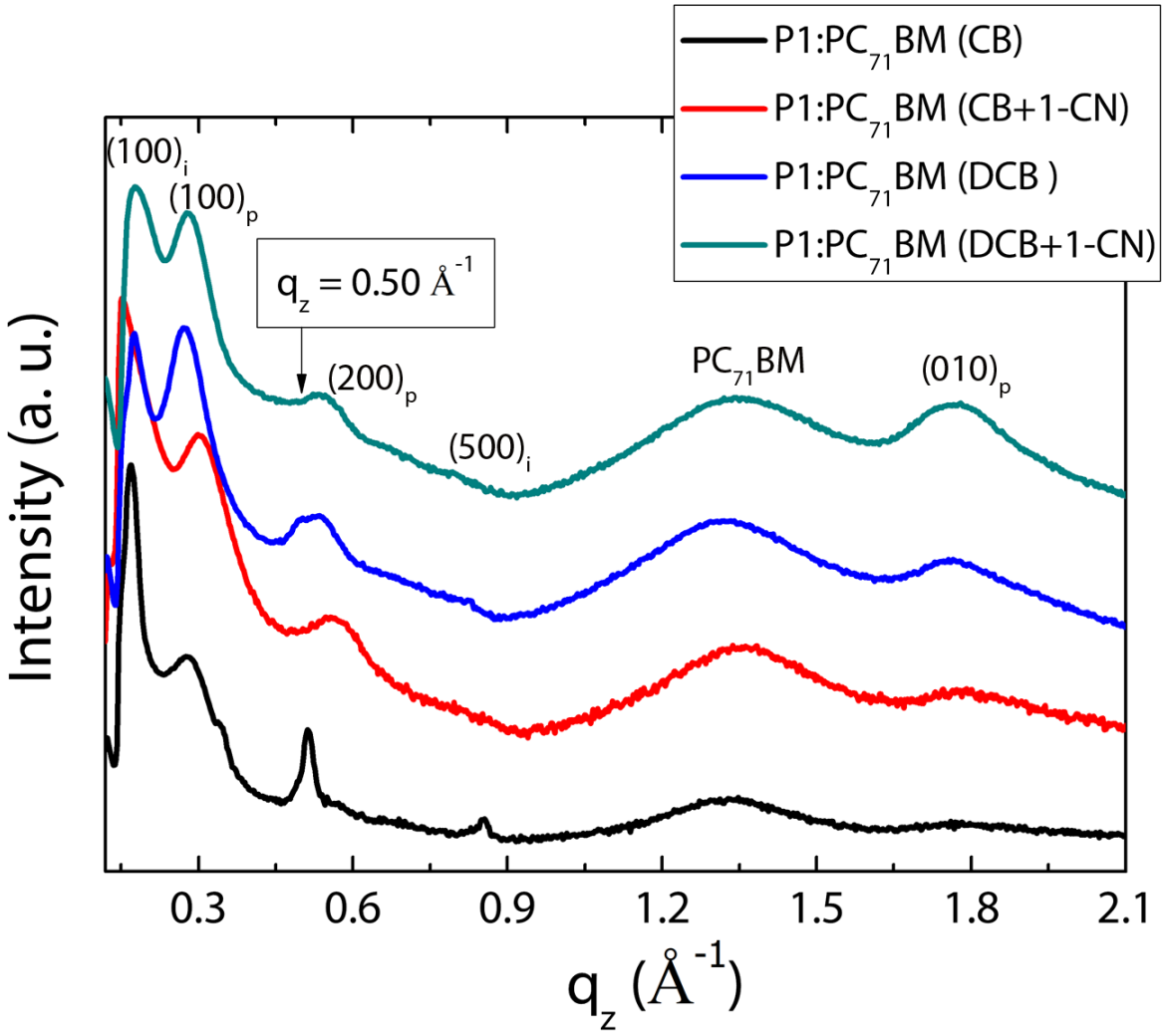

Figure S3. Profile plots of GIWAXS measurement of the P1:$PC_{71}BM$ obtained by spin-casting procedure from solvents of CB (black-line), CB+1-CN (red-line), DCB (blue-line) and DCB+1-CN (dark cyan-line) at a substrate temperature of 25 ºC (out-of-plane direction).

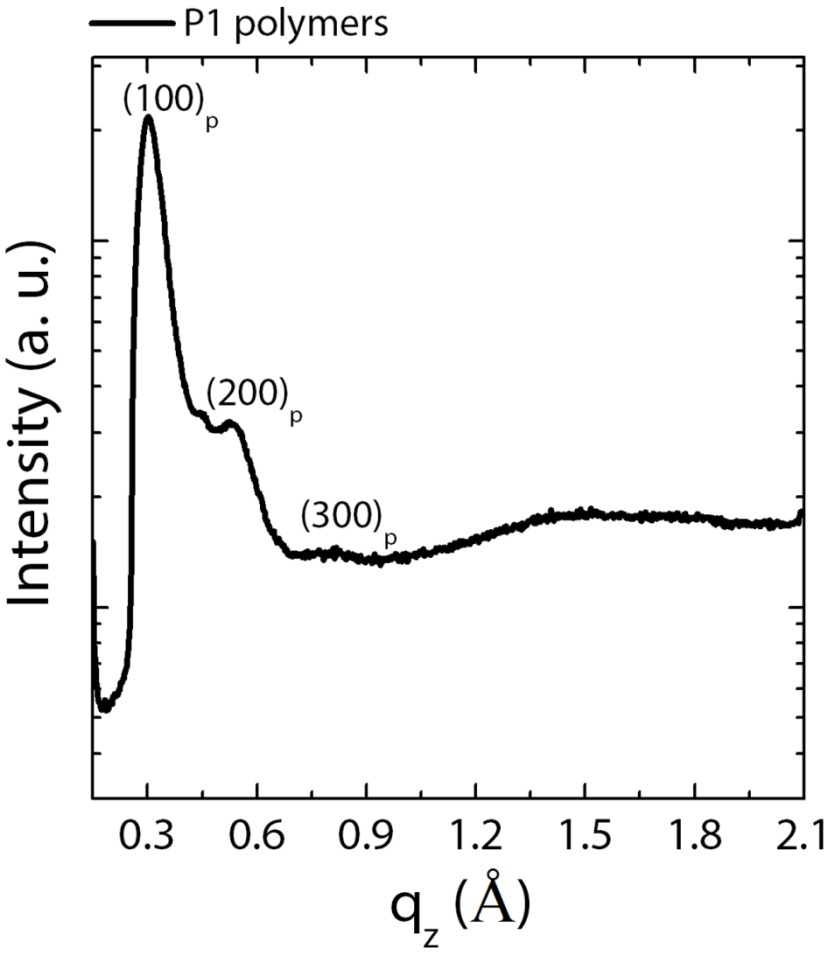

Figure S4. 1D plot of pristine P1 polymer film in out-of-plane direction from GIWAXS measurement.

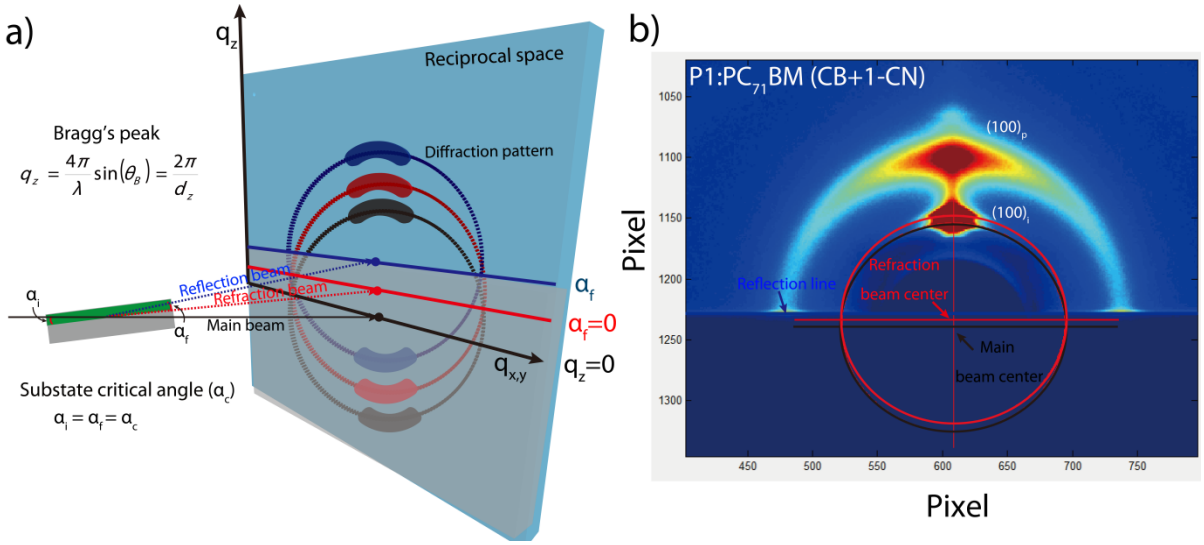

Figure S5. a) Schematic image of GIWAXS measurement at critical angle and b) the 2D GIWAXS pattern of drop-casting P1:$PC_{71}BM$ (CB+1-CN) after 40 minutes, indicating the separated diffraction peak at $(100)_i$ plane is attributed to the refraction beam effect.

In this study, all GIWAXS pattern of drop-casting P1:$PC_{71}BM$ blend were obtained at substrate critical angle (α_c), ~ 0.14°, which is the angle of incidence above which total internal reflection occurs. Thus, both refraction and reflection can occur at the substrate boundary as shown in Figure S5a. As we obtained a main beam center and a reflection line from the measurement, the refraction beam center could be defined as shown in Figure S5b. We found that the position of diffraction pattern by the refraction beam is identical to that of the separated diffraction peak of $(100)_i$ peak although there is no effect of reflection beam.

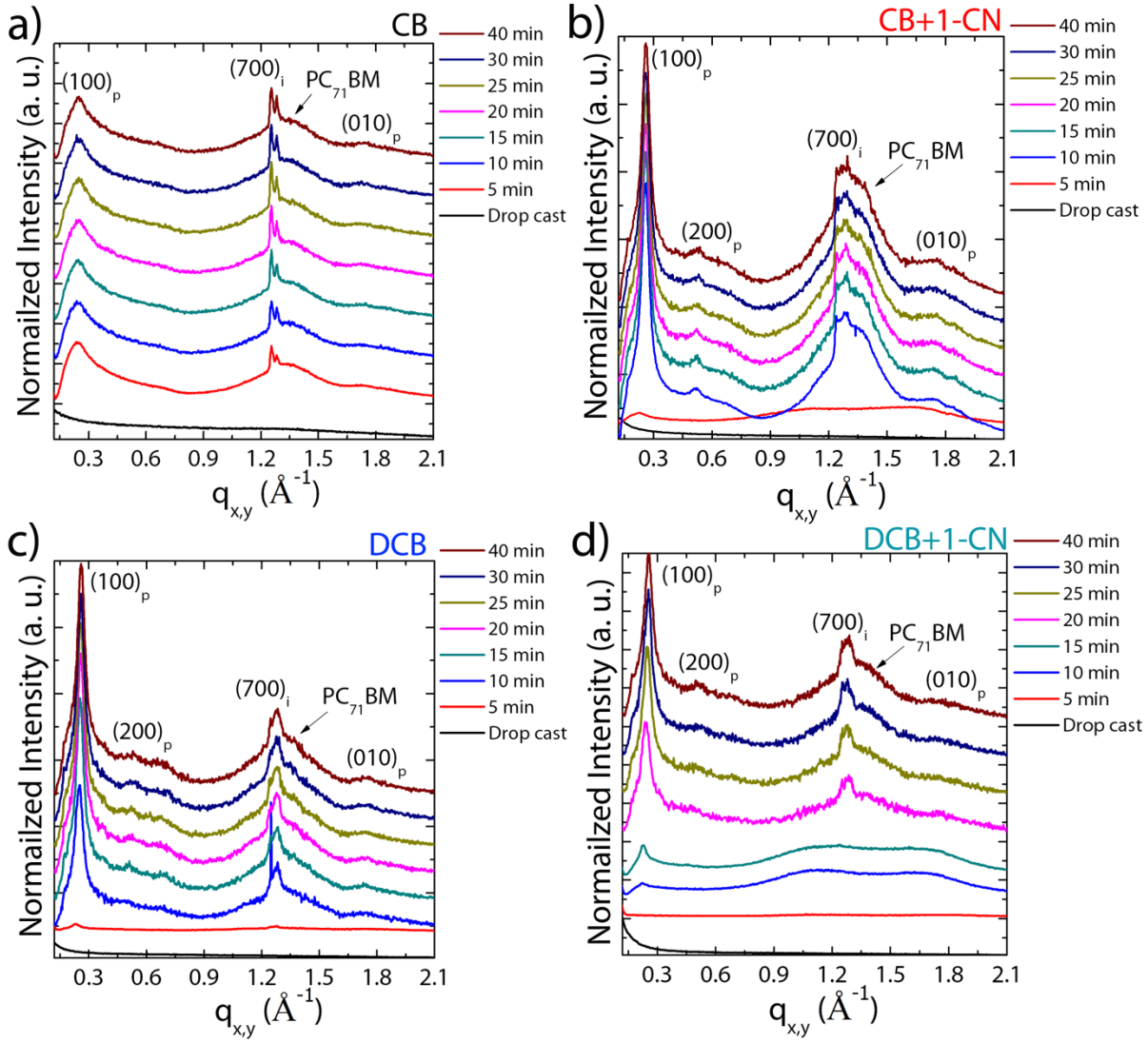

Figure S6. Profile plots of real-time GIWAXS measurement of the P1:$PC_{71}BM$ solution cast from solvents of a) CB, b) CB+1-CN, c) DCB and d) DCB+1-CN at a substrate temperature of 25 ºC (in-plane direction).

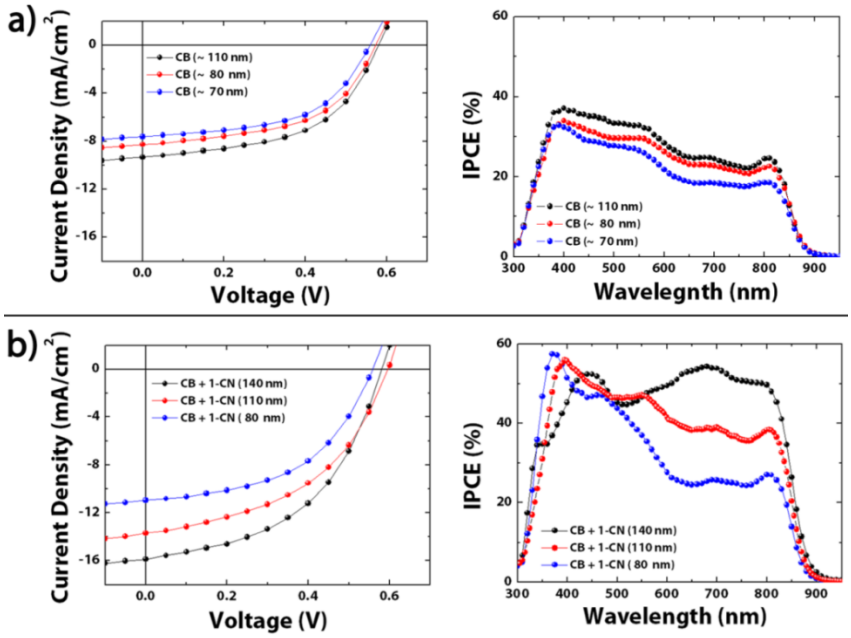

Figure S7. The *J-V* and the corresponding IPCE characteristics of the P1:$PC_{71}BM$ BHJ solar cells with CB and CB + 1-CN solvents at specific thicknesses of the BHJ layer.

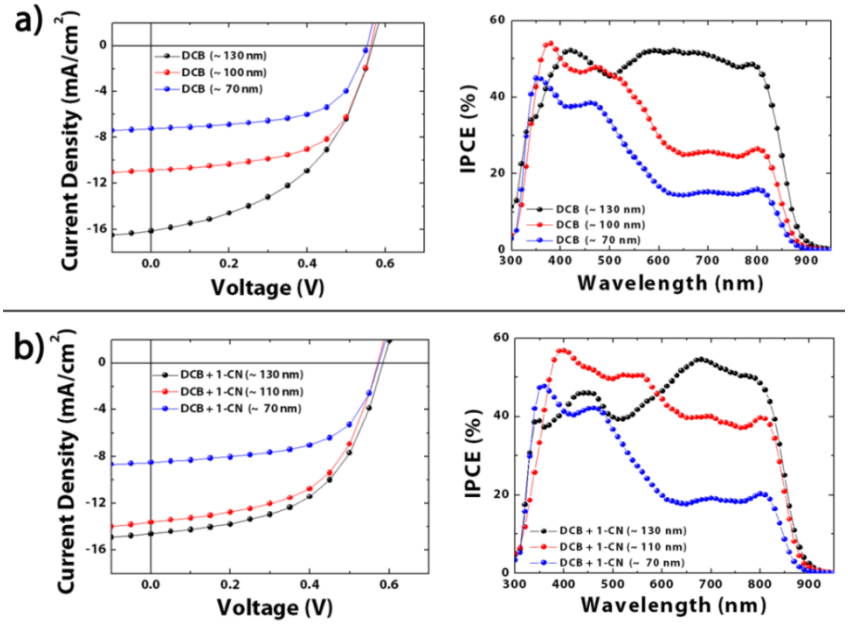

Figure S8. The *J-V* and the corresponding IPCE characteristics of the P1:$PC_{71}BM$ BHJ solar cells with DCB and DCB + 1-CN solvents at specific thicknesses of the BHJ layer.

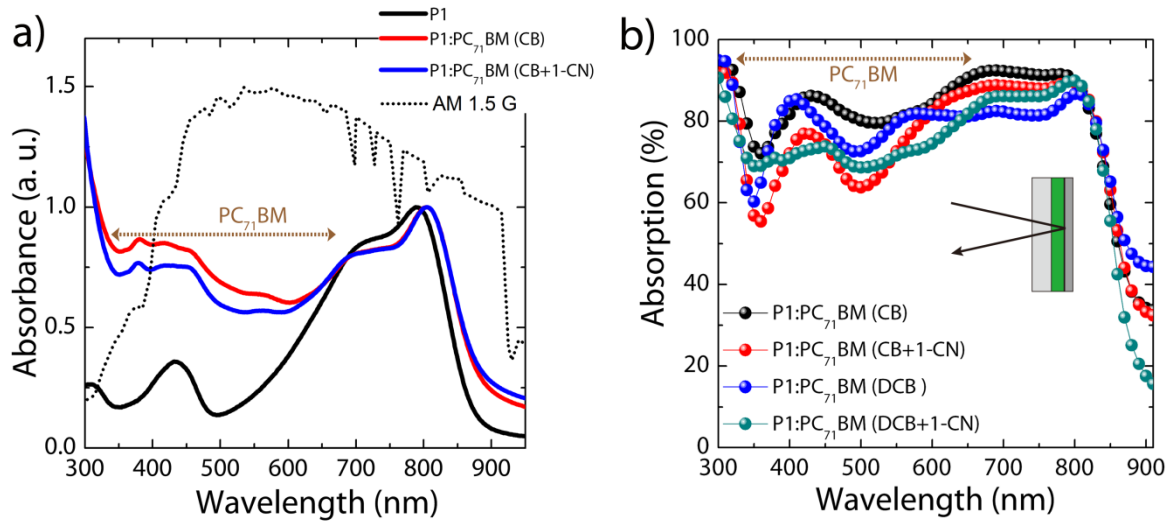

Figure S9. a) The absorption spectra of the pristine P1 polymer and P1:$PC_{71}BM$ BHJ blend film compared with the solar spectrum. b) The reflection absorption spectra of P1:$PC_{71}BM$ films by device geometry.

The absorption spectra of the pristine P1 polymer and P1:$PC_{71}BM$ blend are shown in Figure S9a. The P1 polymer (black line) exhibits a clear vibronic peak at 820 nm and a broad π-π* absorption feature with a narrow optical band gap of 1.4 eV, both of which indicated strong intermolecular interactions between the polymers. The absorption spectra of the P1:$PC_{71}BM$ cast from CB with and without the 1-CN additive are almost identical in the wavelength range of 650–900 nm. However, with the addition of a small amount of 1-CN, the absorption of P1:$PC_{71}BM$ film in wavelength range of 650–300 nm is slightly reduced as compared to that of non-additive case since the 1-CN would remove some portion of $PC_{71}BM$ out of the film due to the high $PC_{71}BM$ solubility of 1-CN (see $PC_{71}BM$ absorption range (brown arrow)). Similar trends were also found in the reflection absorption measurement as shown in Figure S9b, implying that some amount of 1-CN and slow film drying could change the blend ratio of BHJ component. Furthermore, because of the different surface and internal

morphology by various solvent systems as confirmed by the TEM measurement, it would be expected that the electric field distribution is modified within the BHJ film, resulting in the interesting change of internal quantum efficiency (IQE).

Table S1. The photovoltaic performance data for P1:$PC_{71}BM$ with the CB and CB + 1-CN solvents at specific thicknesses.

Solvents	Samples	J_{sc} (mA/cm^2)	V_{oc} (V)	*FF*	η_e (%)
CB	**P1**:**$PC_{71}BM$** ($t \approx 110$ nm)	9.30	0.58	0.53	2.90
	P1:**$PC_{71}BM$** ($t \approx 80$ nm)	8.30	0.57	0.53	2.50
	P1:**$PC_{71}BM$** ($t \approx 70$ nm)	7.60	0.56	0.55	2.30
CB + 1-CN	**P1**:**$PC_{71}BM$** ($t \approx 140$ nm)	15.7	0.59	0.48	4.40
	P1:**$PC_{71}BM$** ($t \approx 110$ nm)	13.8	0.59	0.48	3.90
	P1:**$PC_{71}BM$** ($t \approx 80$ nm)	11.0	0.56	0.50	3.10

Table S2. The photovoltaic performance data for P1:$PC_{71}BM$ with the DCB and DCB + 1-CN solvents at specific thicknesses.

Solvents	Samples	J_{sc} (mA/cm^2)	V_{oc} (V)	*FF*	η_e (%)
DCB	**P1**:**$PC_{71}BM$** ($t \approx 130$ nm)	16.1	0.57	0.48	4.40
	P1:**$PC_{71}BM$** ($t \approx 100$ nm)	11.5	0.56	0.61	3.90
	P1:**$PC_{71}BM$** ($t \approx 70$ nm)	7.20	0.55	0.61	2.40
DCB + 1-CN	**P1**:**$PC_{71}BM$** ($t \approx 130$ nm)	14.6	0.58	0.54	4.60
	P1:**$PC_{71}BM$** ($t \approx 110$ nm)	13.6	0.57	0.55	4.30
	P1:**$PC_{71}BM$** ($t \approx 70$ nm)	8.50	0.57	0.59	2.90